forests

MDPI

Article

Short-Term Effects of Thinning on Stand Carbon Density and Sediment Carbon Burial Indicators in *Kandelia obovata* Sheue & al. Plantation

Shuangshuang Liu [1,2], Xing Liu [1,2], Qiuxia Chen [1,2], Wenzhen Xin [1,3], Sheng Yang [1,2,*] and Jinwang Wang [1,*]

[1] Zhejiang Institute of Subtropical Crops, Zhejiang Academy of Agricultural Sciences, Wenzhou 325005, China; liuss@zaas.ac.cn (S.L.); liuxing@zaas.ac.cn (X.L.); chenqx@zaas.ac.cn (Q.C.); xinwenzhen97@gmail.com (W.X.)
[2] Wenzhou Key Laboratory for Innovative Utilization of Plant Resources, Wenzhou 325005, China
[3] College of Forestry, Beijing Forestry University, Beijing 100083, China
* Correspondence: yangs@zaas.ac.cn (S.Y.); wangjw@zaas.ac.cn (J.W.)

Abstract

To explore the patterns of biomass accumulation and sediment carbon burial indicators in mangrove forests under different thinning intensities, a study was conducted on an 8-year-old *Kandelia obovata* Sheue & al. plantation on Shupaisha Island, Longwan District, Wenzhou City, Zhejiang Province. Three treatments were designed: no thinning (CK), 20% thinning, and 40% thinning. Stand growth and plant carbon density were evaluated for all three treatments at the initial thinning stage and two years later. Sediment carbon density and organic carbon burial rate were assessed only for CK and 20% thinning. Thinning significantly enhanced mangrove growth and plant carbon storage. Compared with unthinned stands, 20% and 40% thinning treatments significantly increased branch diameter and biomass ($p < 0.05$). The order of mangrove height was 20% thinning > 40% thinning > CK. The plant carbon densities in the 20% and 40% thinned stands were 16.31 Mg C·ha^{-1} and 15.30 Mg C·ha^{-1}, respectively, far exceeding that of the control (4.80 Mg C·ha^{-1}). In contrast, sediment carbon responses were negative in the short term. After thinning, the sedimentation rate and organic carbon content in mangrove sediments decreased. Sediment carbon density decreased from 88.10 Mg C·ha^{-1} in unthinned stands to 85.02 Mg C·ha^{-1} under 20% thinning, accompanied by a reduction in carbon burial rate. Overall, these two-year results indicate increased plant carbon storage under thinning, whereas measured sediment carbon indicators under moderate thinning declined over the same period. Longer-term monitoring is needed to assess whether these short-term responses translate into net ecosystem carbon consequences.

Keywords: thinning; mangrove; carbon density; carbon burial

Check for updates

Academic Editor: Marcelo Cancela Lisboa Cohen

Received: 23 December 2025
Revised: 25 February 2026
Accepted: 3 March 2026
Published: 13 March 2026

Copyright: © 2026 by the authors. Licensee MDPI, Basel, Switzerland. This article is an open access article distributed under the terms and conditions of the Creative Commons Attribution (CC BY) license.

1. Introduction

Forests encompass 31% of the worldwide land surface and account for 56% of the global carbon storage, making them the most important carbon sink in terrestrial ecosystems [1,2]. However, since the frequency of forest disturbances has increased globally, forest productivity has gradually decreased, large-scale forest mortality has increased, and forest ecosystem services have become more vulnerable [3]. Thinning is a frequent forest management strategy in silviculture that controls stand density, structure, and species composition, lowering the risk of damage from various disturbances [4,5]. Thinning accounts for approximately 51% of forest management worldwide [6,7].

Reasonable thinning intensity promotes uniform tree growth, optimizes stand spatial structure, enhances forest plant community diversity, and increases forest ecosystem stability, all of which improve stand quality [8]. Research indicates that heavy thinning (≥50%) improves red pine tree growth, flowering, and seed output [9]. Similarly, studies show that higher-intensity thinning (50% intensity) is better suited to producing large-diameter timber in middle-aged artificial red spruce stands [10]. Thinning improves overall stand growth and vitality while also reducing forest mortality and production losses due to insect and pathogen infestations [3]. Thinning affects carbon sequestration capability by altering forest microclimate and soil physicochemical properties [7,11]. According to studies, thinning enhances carbon stock accumulation by creating a more open forest canopy and allowing understory plants to collect soil organic matter [12–15]. Soil organic carbon stocks are essentially determined by forest productivity, litter decomposition, plant fine roots, the binding of soil organic carbon (SOC) to mineral soil, and subsequent losses via mineralization or respiration [11]. Ma et al. [12] found that moderate thinning (30%) increased SOC, whereas 15% and 50% thinning intensities had no significant impact on SOC in *Larix gmelinii* (Rupr.) Kuzen plantations in the third and fourth years following thinning. However, some research shows that thinning has a negative influence on sediment organic carbon reserves [16]. Thinning can reduce soil organic carbon by reducing litter intake, affecting soil structural stability, improving soil microbial activity, and promoting microbial respiration [17,18].

Importantly, however, these findings from temperate or boreal terrestrial plantations provide general context and cannot be directly extrapolated to mangrove ecosystems, where tidal hydrology, sediment biogeochemistry, and root-mediated particle trapping fundamentally shape carbon pathways. Mangrove forests are essential ecosystems in tropical and subtropical coastal intertidal regions, serving ecological tasks such as encouraging sedimentation and land formation, shielding against wind and waves, purifying water bodies, and sustaining biodiversity. They are known as "coastal guardians" and "green lungs of the ocean" [19]. However, frequent human disturbances and insufficient scientific management make mangrove ecosystems extremely vulnerable to degradation [20]. Mature mangrove trees dominate communities, greatly inhibiting seedling growth and preventing population renewal [21]. A GIS-based spatial structure optimization model for mangrove stands demonstrated improved spatial organization in managed regions after thinning operations [20]. These studies indicate the relevance of thinning to mangrove management goals, yet empirical evidence quantifying how thinning influences both plant carbon pools and sediment carbon-related processes in mangrove ecosystems remains limited.

In comparison to coastal ecosystems like seagrass beds and salt marshes, mangroves have well-developed root systems that effectively collect organic-rich floating particles [22]. Anaerobic conditions also slow the breakdown of collected organic particles, which promotes sediment organic carbon burial [23–25]. Given these distinctive mechanisms, thinning-induced changes in canopy structure and root systems may have contrasting effects on plant carbon accumulation versus sediment carbon burial, but such responses are still insufficiently resolved. *Kandelia obovata* Sheue & al. is the most widely spread, northernmost, and cold-tolerant genuine mangrove species in China, with the northernmost artificial distribution recorded at Ximen Island in Yueqing, Zhejiang Province (28°20′ N) [26]. After years of introduction and acclimatization, *K. obovata* has emerged as the principal mangrove afforestation species in Zhejiang Province. It should be noted that *K. obovata* in Zhejiang Province is influenced by temperature, often exhibiting a dwarf shrub or low forest form, which is markedly different from the tall tree-type mangroves found in tropical regions. Therefore, this study focuses on an 8-year-old *K. obovata* plantation located on Shupaisha Island in Longwan District, Wenzhou City, Zhejiang Province. This research

aims to lay the groundwork to improve mangrove carbon sequestration capacity through improved silvicultural management by investigating the effects of different thinning intensities on growth parameters, plant carbon density, and sediment carbon burial rates, as well as to provide scientific guidelines for the conservation and sustainable management of mangrove wetlands.

2. Materials and Methods

2.1. Study Area

The study site is situated on Shupaisha Island in Longwan District, Wenzhou (120°50′56″–120°52′20″ E, 27°56′39″–27°57′30″ N). The mangrove forest on Shupaisha Island lies within the Oujiang River estuary, part of the Wenzhou Bay international important wetland, which was declared the Zhejiang Provincial Marine Special Protection Area in 2019. Mangrove restoration efforts began in 2014, and the current mangrove area spans approximately 67 hectares, dominated by *K. obovata*. The stand characteristics include an average tree height of 117.78 cm, an average crown spread of 1.18 m^2, a canopy cover of 86.38%, and an average density of 0.92 plants per square meter (Figure 1).

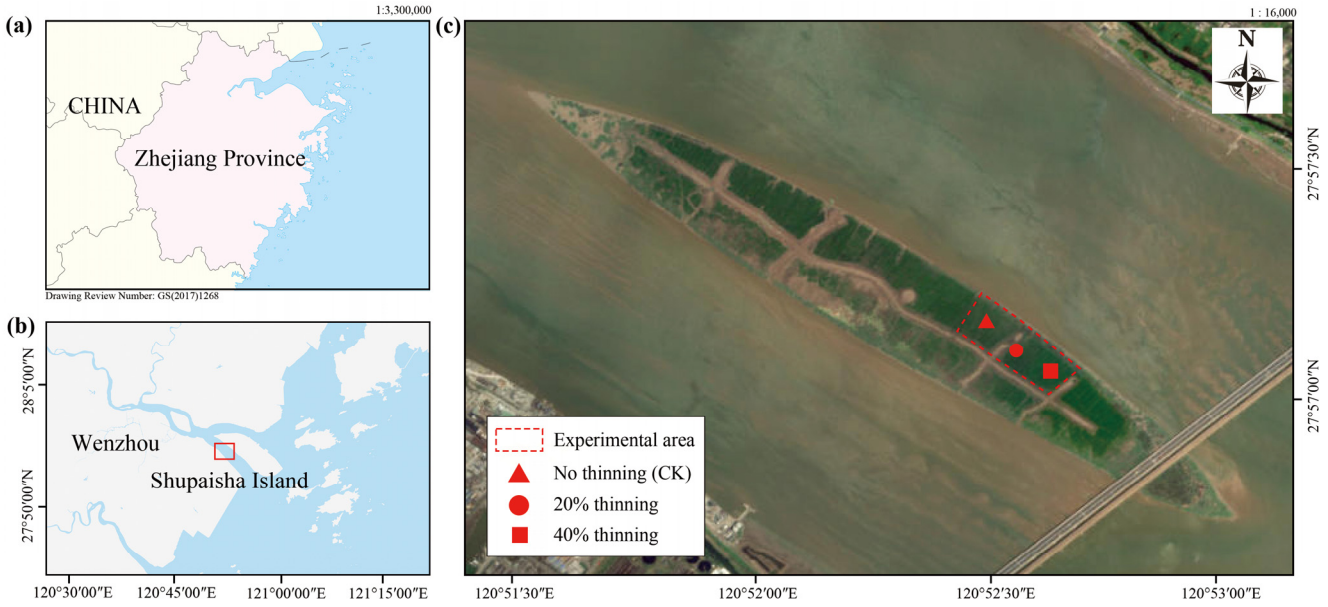


Figure 1. Distribution map of survey plots in Shupaisha Island mangrove forest. (**a**) Location of the study area in China. (**b**) Sampling island in Wenzhou. (**c**) Sampling sites of three treatments in Shupaisha Island.

2.2. Experimental Design

In 2022, eight-year-old *K. obovata* stands with densities exceeding 2 plants per square meter on Shupaisha Island, Longwan, were chosen as study subjects. The island-wide mean density (0.92 plants per square meter) was derived from heterogeneous stand conditions across the entire restoration area, whereas the experimental plots were purposively located in continuous, high-density patches (exceeding 2 plants per square meter) to enable thinning implementation and plot-scale replication. The study area accounts for approximately 9.0% of the total mangrove area on the island (approximately 6 hectares). Three thinning intensities were established: no thinning (CK), 20% thinning, and 40% thinning (Figure 2). The different treatment plots are evenly distributed, with an interval of approximately 100 m. For each treatment, three replicate plots were established, resulting in a total of nine plots. Each plot was 10 m × 10 m in size. Initial plant density before thinning was 2.40 ± 0.10, 2.53 ± 0.09 and 2.47 ± 0.15 plants per square meter in the CK, 20%, and

40% thinning treatments, respectively. The growth conditions of *K. obovata* stands were evaluated at the initial thinning stage in 2022 and two years later in 2024. Plant carbon density was measured, and sedimentation rates as well as sediment organic carbon content were quantified. Given the shrub-like, low-stature growth form and relatively high stem density in Zhejiang, a 100 m^2 plot typically contains sufficient individuals for robust estimation of stand-structure metrics. Sediment physicochemical properties and sediment carbon-related variables were analyzed for the CK and 20% thinning treatments only. The 40% thinning treatment was not included in sediment sampling due to field sampling and laboratory processing capacity constraints.

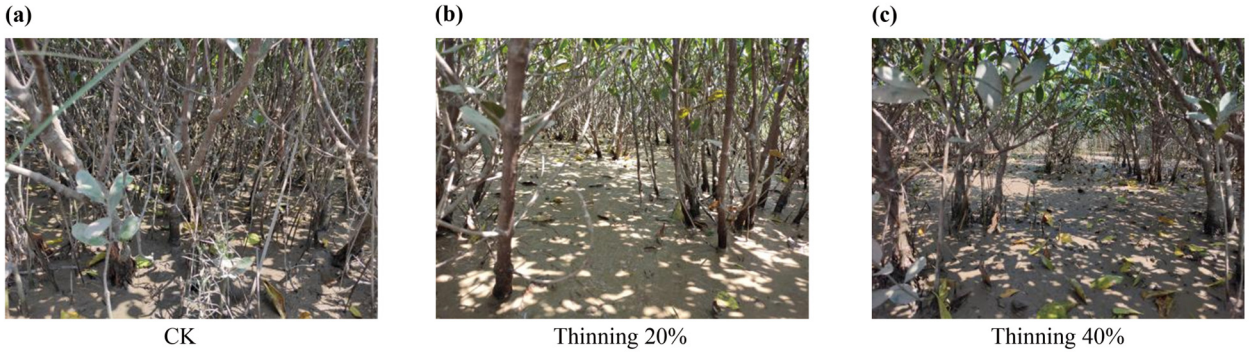


Figure 2. (**a**) CK, (**b**) 20% thinning and (**c**) 40% thinning sample plot photos.

The Shupaisha Island site was selected because it contains a relatively high-density *K. obovata* stand, enabling clear thinning treatments and plot-scale replication. Plot assignment to thinning intensities was not randomized; instead, plots with similar pre-treatment stand structure and site conditions were selected and spaced ~100 m apart to reduce spatial autocorrelation. We acknowledge that selecting a high-density stand may limit broader representativeness; therefore, results should be interpreted as treatment responses within this site.

2.3. Plant Community Survey

Growth surveys of *K. obovata* within the plots were conducted at the start of thinning and two years post-thinning. Three 10 m × 10 m plots were established within each mangrove plant plot to assess the height and branch diameter (diameter measured at one-tenth of the stem length near ground level) of *K. obovata*.

2.4. Estimation of Mangrove Plant Carbon Stock

The biomass of individual mangrove plants (including aboveground biomass and belowground biomass) was calculated using a species-specific allometric equation developed by our research team [27]. This equation was selected because it has been reported to be applicable to the structural characteristics of *K. obovata* in Zhejiang Province. The selected allometric equation does not explicitly include wood density as an input variable, as species-specific structural characteristics are implicitly incorporated into the fitted coefficients. The formula is as follows:

$$W_T = 3.614 \times D^{1.446} \quad (1)$$

where W_T represents individual biomass (g), and D represents branch diameter (mm).

Plant carbon density was estimated by multiplying the biomass per unit area within the plot by the species-specific carbon density coefficient. The carbon conversion coefficient for *K. obovata* is 0.423. This value was adopted based on local empirical measurements

and previous project datasets. All ha units in this study are area-standardized (areal density) and are converted based on a 10 m × 10 m plot. The specific calculation formula is as follows:

$$VC_P = W_T \times D_P \times \varphi \times 100 \quad (2)$$

In the equation, VC_P represents plant carbon density (Mg C·ha^{-1}), W_T denotes individual biomass (g), D_P indicates plant density (plants·m^{-2}), and φ is the carbon conversion coefficient.

The biomass equation assumes that tree form and biomass allocation of *K. obovata* in the study area are comparable to those used in the original model calibration. The use of a constant carbon conversion coefficient assumes limited variation in woody tissue carbon content across thinning treatments. The carbon conversion coefficient can vary with organ type and growth conditions, and thinning-related changes in microclimate and growth could cause small shifts in carbon concentration. These assumptions may affect absolute carbon stock estimates but are unlikely to influence relative comparisons among treatments over the two-year period.

2.5. Determination of Sediment Physicochemical Properties

In 2024, two years after thinning of *K. obovata*, surface sediments from the 0–20 cm depth in each plot were collected for physicochemical property analysis. Soil pH was measured using a pH meter. Total nitrogen content was determined using the Kjeldahl method, and total phosphorus content was measured by alkali fusion molybdenum–antimony (Mo–Sb) anti-spectrophotometric method. Total carbon content was determined by the sodium hydroxide alkali fusion Mo–Sb anti-spectrophotometric method, while sediment organic carbon content was measured using the potassium dichromate oxidation–reduction titration method. Available nitrogen was determined using the diffusion method, available phosphorus was measured by the Mo–Sb anti-spectrophotometric method, and total soluble salt was determined using the gravimetric method.

Simultaneously, a soil sampler was used to collect one 1 m-deep sediment column sample from each plot (three treatments × three plots, n = 9), with no significant vertical compression. After collection, the samples were stratified into seven layers: 0–10 cm, 10–20 cm, 20–30 cm, 30–40 cm, 40–50 cm, 50–70 cm, and 70–100 cm. Each layer was sealed, labeled, and transported to the laboratory for storage and subsequent analysis. For each layer, dry weight (g), volume (cm^3), and sediment organic carbon content were measured separately.

2.6. Determination of Organic Carbon Burial Rate and Sediment Carbon Density

In 2022, sedimentation rate markers were installed in mangrove plots under two treatments: no thinning and 20% thinning. Within each plot, areas with relatively gentle topography were selected to obtain sedimentation rates using the horizontal marker layer method. White putty powder was scattered over the selected gentle slope areas. After two years, the top portion of a disposable syringe barrel was cut off with a small knife, retaining the main barrel and piston sections. The remaining syringe was inserted into the sediment layer of the mangrove mudflat where plaster powder had been scattered. A soil column was then extracted from the syringe, which consisted of three distinct layers: Layer A (older sediment), Layer B (plaster powder layer), and Layer C (sediment formed by tidal erosion). The vertical distance between the upper surface of Layer B (plaster powder) and the upper surface of Layer C (tide-eroded sediment) was measured using a ruler with 1 mm resolution and defined as height H. Three independent marker-horizon measurements were collected per plot (i.e., three syringe cores from three locations). The plot-level H was calculated as the mean of the three measurements, and within-plot variability was quantified as the

standard deviation (SE) among the three cores. The sediment accumulation rate (SAR) of the mangrove over the two-year period was calculated as (C − B)/2, i.e., H/2.

The organic carbon burial rate and sediment carbon density are calculated according to Lyu et al. [25], using the following formula:

$$OCAR = BD \times C_{org} \times SAR \times 0.1 \quad (3)$$

$$C = BD \times C_{org} \times H \times 0.1 \quad (4)$$

where $OCAR$ is the organic carbon burial rate (Mg C·ha^{-1}·a^{-1}), BD is the sediment bulk density (g·cm^{-3}), C_{org} is the organic carbon content (g·kg^{-1}), SAR is the sedimentation rate (mm·yr^{-1}). C is the organic carbon density (Mg C·ha^{-1}), and H is the sediment thickness (cm). $OCAR$ was calculated at the plot level using plot-specific BD, C_{org}, and SAR values. Treatment-level results are reported as mean ± SE across replicate plots (n = 3). Uncertainty in $OCAR$ was estimated using standard error propagation, assuming independent uncertainties in BD, C_{org}, and SAR.

2.7. Statistical Analysis

Data statistics and graphical analysis were performed using Excel 2016, and values are presented as mean ± SE. Baseline measurements were used to verify pre-treatment similarity among plots, whereas post-thinning comparisons and changes from baseline were used to evaluate treatment-level differences. One-way ANOVA and Duncan's multiple range test were conducted using SPSS 25.0, with $p < 0.05$ set as the significance level. Prior to ANOVA, the assumptions of normality and homoscedasticity were evaluated using the Shapiro–Wilk test and Levene's test, respectively.

3. Results

3.1. Differences in Mangrove Community Structure Under Different Thinning Intensities

At the initial stage of thinning, differences existed among treatments in the height, branch diameter, and single plant biomass of *K. obovata*. Higher thinning intensities correlated with lower plant height, branch diameter, and single plant biomass. Specifically, the 20% and 40% thinning treatments exhibited significantly lower branch diameter and individual biomass compared to the unthinned control (Figure A1; Table A1).

Two years after thinning, the height, branch diameter, and biomass of *K. obovata* in all thinned treatments surpassed those of the control. The height of *K. obovata* in the 20% and 40% thinned stands increased by 21.82% and 2.45%, respectively, relative to the control. The 20% thinning stand exhibited the greatest height at 186.36 cm, significantly exceeding the control. Branch diameter also increased, with both the 20% and 40% thinned plots showing significantly greater branch diameter than the unthinned plot. A similar trend was observed for biomass. In the 20% and 40% thinned plots, plant biomass reached 1010.63 g and 1173.84 g, respectively—both values significantly exceeding that of the unthinned control (Figure A1; Table A1). These treatment differences are based on the post-thinning (2024) absolute values.

Additionally, two years after thinning, height in all thinning treatments showed marked increases compared to the initial stage. Under 20% and 40% thinning, height increased significantly by 63.89 cm and 57.10 cm, respectively. Across all thinning intensities, both branch diameter and individual plant biomass increased significantly ($p < 0.001$) two years post-thinning compared to initial measurements, indicating a strong recovery and growth response following thinning (Figure A1; Table A1).

Two years after thinning, growth increment data reveal that mangrove height, branch diameter, and biomass growth under different thinning intensities were significantly higher

compared to unthinned stands. For *K. obovata*, height growth in the CK, 20% thinning, and 40% thinning treatments reached 29.38 cm, 63.89 cm, and 57.10 cm, respectively, with 20% > 40% > CK. Thinning significantly enhanced height growth ($p < 0.05$). After two years, branch diameter growth of *K. obovata* increased progressively with thinning intensity. The 40% thinning treatment resulted in the highest branch diameter increment at 39.11 mm, followed by the 20% thinning treatment at 33.79 mm—representing increases of 2.26-fold and 1.82-fold compared to the CK, respectively. Biomass and branch diameter growth showed similar trends, with both 20% and 40% thinning treatments exhibiting significant enhancements in biomass accumulation ($p < 0.001$) (Figure A2). These results indicate that thinning, particularly at a moderate intensity, effectively promotes structural growth and biomass production in *K. obovata* stands. The growth increments represent changes from baseline and were used to account for baseline differences among plots.

3.2. Carbon Density of Mangrove Plants Under Different Thinning Intensities

To address stand-level responses relevant to forest management, we further compared stand biomass and plant carbon density, which explicitly account for the combined effects of tree growth and thinning-induced changes in density. Thinning intensity had a significant effect on stand biomass. Initially, the unthinned stand had the lowest biomass at 4.99 Mg·ha^{-1}, whereas the 20% thinning treatment achieved the highest biomass at 8.93 Mg·ha^{-1}. The plant carbon densities in the unthinned, 20% thinned, and 40% thinned stands were 2.11 Mg C·ha^{-1}, 3.78 Mg C·ha^{-1}, and 3.47 Mg C·ha^{-1}, respectively. Two years after thinning, the plant carbon density in *K. obovata* stands subjected to 20% and 40% thinning was significantly higher than in the unthinned stand. Notably, the 20% thinned stand exhibited the highest plant carbon density, reaching 3.40 times that of the unthinned stand. The unthinned stand still had the lowest biomass at 11.35 Mg·ha^{-1}, while the 20% thinned stand maintained the highest biomass at 38.55 Mg·ha^{-1}—slightly greater than the 36.16 Mg·ha^{-1} recorded in the 40% thinned stand and substantially higher than the unthinned control (Figure 3; Table 1). After two years, both biomass and plant carbon density in all thinned *K. obovata* stands increased significantly ($p < 0.01$) compared to pre-thinning levels.

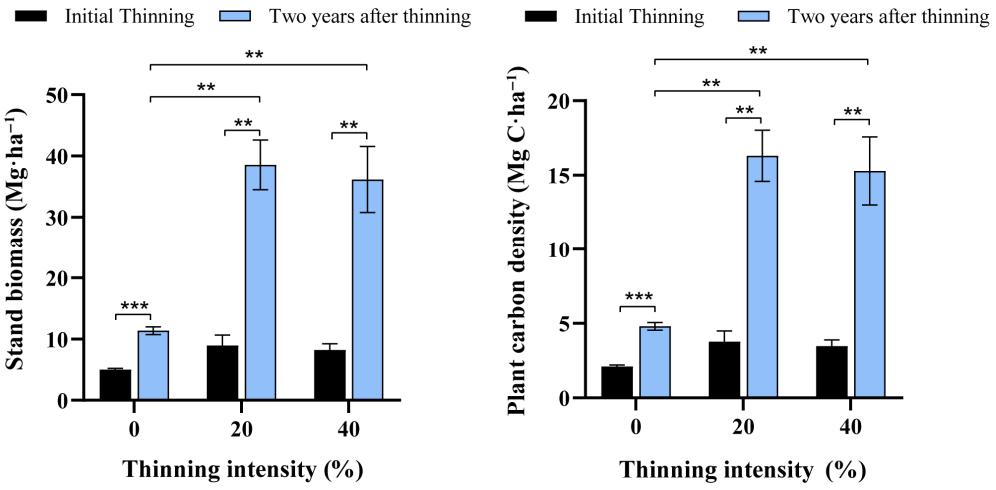


Figure 3. Plant carbon density in mangrove forests under different thinning intensities. Asterisks indicate significant pairwise differences as shown by the brackets (** $p < 0.01$, *** $p < 0.001$).

Table 1. Plant carbon density at the initial thinning stage and two years after thinning under different thinning intensities.

Time Point	Thinning Intensity (%)	Stand Biomass ($Mg \cdot ha^{-1}$)	Plant Carbon Density ($Mg\ C \cdot ha^{-1}$)
Initial thinning	0	4.99 ± 0.22	2.11 ± 0.10
	20	8.93 ± 1.70	3.78 ± 0.72
	40	8.19 ± 1.02	3.47 ± 0.43
Two years after thinning	0	11.35 ± 0.61	4.80 ± 0.26
	20	38.55 ± 4.05	16.31 ± 1.71
	40	36.16 ± 5.40	15.30 ± 2.29

Note: Values are means ± SE (n = 3 plots per treatment). 0% thinning intensity denotes the unthinned control (CK). Units are shown in column headers.

While Table 1 and Figure 3 summarize post-thinning absolute values, Figure 4 presents changes from baseline values, which were used to account for baseline differences among treatments. The increase in stand biomass of *K. obovata* two years after thinning followed a trend of initial increase subsequent to a decline as thinning severity increased. Compared to the unthinned control, all thinned treatments resulted in significantly greater biomass accumulation, with the 20% thinning treatment achieving the highest value of 29.62 $Mg \cdot ha^{-1}$. However, there was no discernible difference in biomass increase between the 20% and 40% thinning treatments. A similar pattern was observed for plant carbon density growth. Two years post-thinning, the 20% and 40% thinned stands did not differ significantly in carbon density growth, although both were considerably greater than the control. The 20% thinning treatment showed the greatest plant carbon density growth, reaching 12.53 $Mg\ C \cdot ha^{-1}$ (Figure 4).

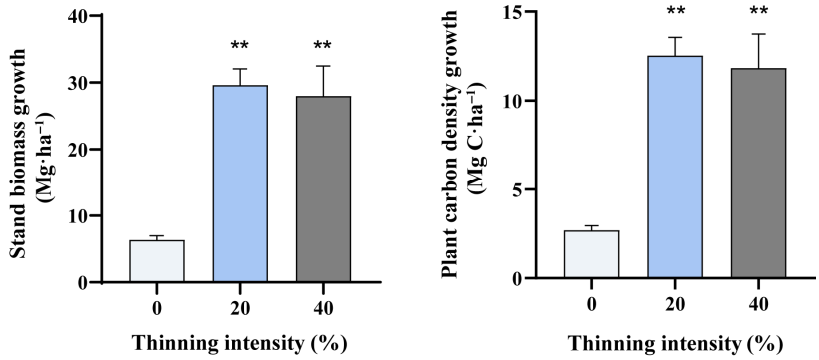


Figure 4. Changes in mangrove plant carbon storage under different thinning intensities. Asterisks indicate significant differences compared with the control (** $p < 0.01$).

3.3. Sediment Physicochemical Properties of Mangroves Under Moderate Thinning

Soil pH showed little change between undisturbed and 20% thinned plots, with values of 7.35 and 7.32, respectively, indicating a broadly stable acidity/alkalinity environment following thinning. However, following thinning, total nitrogen, total carbon, and soluble total salt content increased compared to the undisturbed condition, with soluble total salt showing a particularly pronounced increase. In contrast, available nitrogen and available phosphorus decreased after thinning, with reductions of 2.49 $mg \cdot kg^{-1}$ and 1.90 $mg \cdot kg^{-1}$, respectively (Figure A3). These observations provide only tentative indications that total pools and plant-available forms may respond differently in the short term, and they were therefore not used as primary evidence for sediment carbon interpretations.

The bulk density of sediment from the Shupaisha Island mangroves ranged from 0.84 $g \cdot cm^{-3}$ to 1.20 $g \cdot cm^{-3}$ (Figure 5). In unthinned mangrove sediments, bulk density

initially increased with soil depth before decreasing, peaking at 1.20 g·cm^{-3} in the 40–50 cm layer—a 42.86% increase compared to the surface layer (0–10 cm). In contrast, sediments from 20% thinned mangroves exhibited minimal variation in bulk density between 20 cm and 100 cm depths. Across the entire 0–100 cm soil profile, the average bulk density was 1.02 g·cm^{-3} in unthinned mangroves, while it was slightly lower at 1.00 g·cm^{-3} in the 20% thinned treatment (Figure 5).

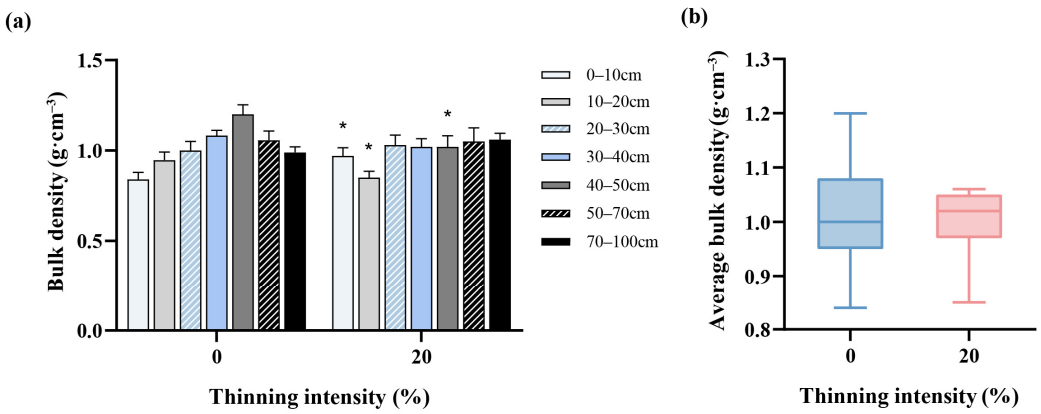


Figure 5. Bulk density of mangrove sediments under moderate thinning. Within the same soil depth, asterisks indicate significant differences between thinning treatments (* $p < 0.05$). If no significant differences were detected for a variable, no letters are shown. (**a**) Soil bulk density of each layer under different thinning intensities. (**b**) Average bulk density under different thinning intensities.

The organic carbon content in sediments from unthinned mangrove forests initially decreased with increasing soil depth before subsequently increasing. In the unthinned plots, SOC decreased from the surface to 20–30 cm and then increased again toward deeper layers, whereas in the 20% thinned plots, SOC generally increased with depth. (Figure 6a). Within the 1 m soil profile, the average organic carbon content in unthinned mangrove sediments was 8.15 g·kg^{-1}, compared to 7.99 g·kg^{-1} in the 20% thinned treatment (Figure 6b), indicating that thinning mainly altered the vertical distribution rather than substantially changing the profile-average SOC over the study period.

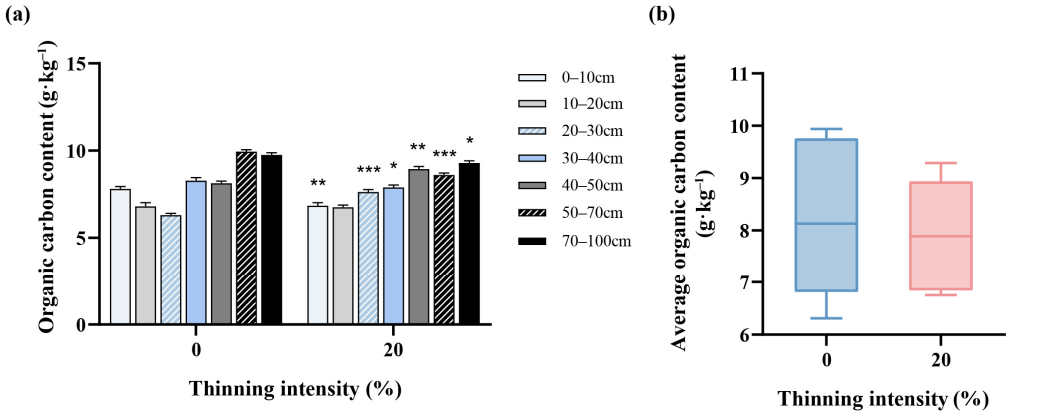


Figure 6. Organic carbon content in mangrove sediments under moderate thinning. Within the same soil depth, asterisks indicate significant differences between thinning treatments (* $p < 0.05$, ** $p < 0.01$, *** $p < 0.001$). If no significant differences were detected for a variable, no letters are shown. (**a**) Organic carbon content of each layer under different thinning intensities. (**b**) Average organic carbon content under different thinning intensities.

3.4. Organic Carbon Burial Rate and Sediment Carbon Density of Mangroves Under Moderate Thinning

Sediment carbon density gradually increased with soil depth, with a notable rise observed when the depth exceeded 50 cm (Table 2). Within the 1 m soil profile, the sediment carbon densities were 88.10 Mg C·ha^{-1} for unthinned mangroves and 85.02 Mg C·ha^{-1} for 20% thinned mangroves, an absolute difference of 3.08 Mg C·ha^{-1}, equivalent to 3.5% relative to the unthinned control, indicating a decrease in sediment carbon density following thinning. Given the small number of replicate plots (n = 3) and the standard errors, this between-treatment difference is modest and should be interpreted cautiously.

Table 2. Sediment carbon density in mangroves under moderate thinning.

Thinning Intensity (%)	Soil Layer Depth (cm)							Sediment Carbon Density (Mg C·ha^{-1})
	0–10	10–20	20–30	30–40	40–50	50–70	70–100	
0	6.65 ± 0.23	6.47 ± 0.13	6.31 ± 0.16	8.94 ± 0.24	9.76 ± 0.33	21.07 ± 0.46	28.99 ± 0.30	88.10 ± 0.98
20	6.63 ± 0.27	5.74 ± 0.09	7.86 ± 0.16	8.05 ± 0.16	9.12 ± 0.38	18.08 ± 0.62	29.54 ± 0.72	85.02 ± 1.33

Note: Values are means ± SE (n = 3). 0% thinning intensity denotes the unthinned control (CK). Units are shown in column headers.

The sedimentation rate was 43.22 mm·yr^{-1} in undisturbed mangroves and 39.89 mm/a in 20% thinned mangroves (Figure 7). Based on these values, the corresponding organic carbon burial rates were calculated to be 35.93 Mg C·ha^{-1}·yr^{-1} and 31.87 Mg C·ha^{-1}·yr^{-1}, respectively. These results demonstrate that within two years after thinning, both sedimentation rate and organic carbon burial rate declined after thinning.

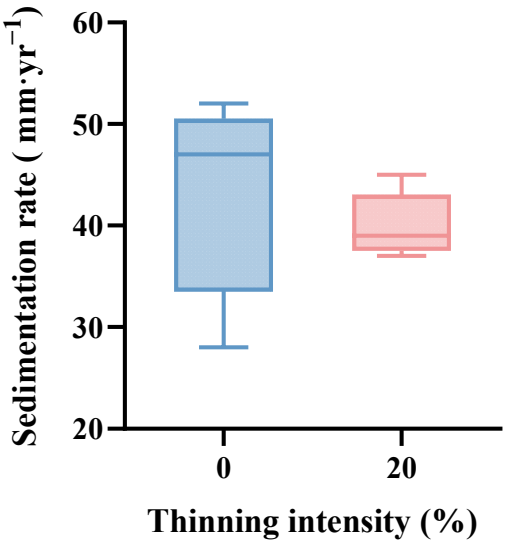


Figure 7. Sedimentation rate of mangrove soils under moderate thinning. Values are mean ± SE across plots (n = 3). Each plot value is based on the mean of three marker-horizon measurements (three cores).

4. Discussion

Forest ecosystems require an optimized stand structure to enhance productivity and timber quality [10]. Extensive research has demonstrated that thinning improves stand structure by removing low-vitality trees, thereby reducing competition for water, nutrients, and light, promoting growth of retained trees, and improving timber quality [10,28–31]. In this study, two years after thinning, height, branch diameter, and biomass of *K. obovata* stands subjected to different thinning intensities were all higher than those in the control. Growth increment data revealed that height, branch diameter, and biomass of *K. obovata* under various thinning intensities were significantly greater compared to unthinned stands.

These findings align with thinning studies on *Quercus mongolica* Fisch. ex Ledeb secondary forests [32], *L. gmelinii* [33], and medium-aged *Toona sinensis* (A. Juss.) Roem stands [34]. The positive effects of thinning are attributed to reduced stand density, which alleviates resource competition and better meets the requirements of individuals for growth space and nutrient availability. Increased inter-tree spacing enhances light penetration within the canopy, improves light use efficiency, promotes lateral branch development, and consequently boosts branch diameter and biomass accumulation [35]. However, some studies report negligible effects of density manipulation on tree growth [36], which may be related to site quality and species-specific biological characteristics [37].

Thinning modifies stand density, thereby enhancing leaf development and diameter growth, which in turn increases overall stand volume [38]. Research has shown that, after 10 years of thinning, carbon stock increments in U.S. national forests significantly increased. Light and moderate thinning treatments were found to effectively improve the tree growth environment, demonstrating strong potential for carbon stock accumulation. Regarding long-term carbon stock accumulation effects, intensive thinning outperformed light thinning treatments, more favorably promoting the accumulation of forest carbon stocks [39]. This study reached similar conclusions: two years after thinning, both 20% and 40% thinned mangrove forests exhibited significantly higher plant carbon density compared to unthinned stands. Specifically, thinned mangrove stands showed marked increases in stand biomass and plant carbon density growth relative to unthinned forests.

Plant density is critical in influencing soil organic carbon content. High-density mangrove stands provide greater amounts of litterfall and exhibit higher net primary productivity. Combined with their extensive fine root systems, these factors contribute to soil organic carbon accumulation [40]. This study indicates that mangrove organic carbon content and sediment carbon density decreased after thinning. Given the pronounced small-scale spatial heterogeneity of mangrove sediments and the limited replication (n = 3), this magnitude should be interpreted as a modest shift rather than definitive evidence of functional degradation. Although sediment carbon density in the 1 m profile was lower under 20% thinning by 3.08 Mg C·ha^{-1} (3.5%), this effect size is modest relative to the substantial natural spatiotemporal variability of mangrove sediments. Soil carbon stocks can vary widely across sites and mangrove community types even within the same region [41], and interannual variability in accretion and organic carbon burial can be comparable to small percentage differences measured over short windows [42]. Therefore, while thinning may alter sediment trapping and surface-elevation dynamics, belowground carbon responses are likely context-dependent, and longer-term monitoring with greater spatial replication is needed before inferring ecosystem-level functional degradation from a 3.5% profile-integrated difference [43]. Research suggests that well-aerated sediments promote microbial growth and activity, accelerating the decomposition and transformation of organic matter. Conversely, sediments with high water retention maintain elevated humidity, facilitating organic matter degradation and fixation, thereby enhancing sediment organic carbon accumulation [44,45]. Following mangrove thinning, increased exposure to oxygen may lead to more oxidizing sediment conditions, potentially accelerating organic matter decomposition and thereby reducing organic carbon content [46]. Additionally, the dense root systems of unthinned mangroves form effective surface barriers that minimize sediment resuspension and lateral transport across tidal flats. These roots also facilitate the trapping and settling of suspended organic particles from the water column, enhancing the capture of exogenous organic carbon [47]. In this study, the organic carbon burial rate in thinned mangroves decreased compared to unthinned stands, which could be partially attributable to reduced sedimentation rates if root stabilization and particle trapping were weakened after thinning. These mechanisms are plausible but remain inferential in

the absence of direct measurements of redox conditions, root biomass and architecture, and particulate trapping; therefore, the differences in sediment carbon indicators should be viewed as preliminary effect sizes over a two-year window rather than evidence of sustained degradation.

Previous studies have shown that the highest soil organic carbon (SOC) content in mangroves may occur at depths of 20–40 cm [48]. However, other studies on mangrove species such as Sonneratia apetala and Aegiceras corniculatum have reported a non-monotonic pattern in which SOC decreases initially and then increases with increasing soil depth [49]. In the present study, SOC generally increased with depth, while bulk density in the unthinned mangrove sediments increased first and then decreased. These two variables exhibited a clear negative relationship in the mid-to-deep soil layers. In the surface-to-mid-depth layers, tidal scouring, alternating wetting and drying, and progressive sediment compaction likely promoted a denser soil structure and higher bulk density. With increasing depth into the mid-to-deep layers, the concurrent decrease in bulk density and increase in SOC may be jointly driven by root inputs and depositional processes. Mangrove species typically develop well-developed vertical root systems that can deliver substantial organic carbon directly into deeper soil layers; root growth, mortality, and subsequent decomposition provide additional SOC inputs [50,51]. Moreover, Shupaisha Island is a typical estuarine sandbar wetland, where frequent depositional events may result in relatively loose, newly deposited sediments in deeper layers that have not yet fully compacted. Such lower bulk density conditions may favor rapid burial and physical isolation of organic carbon. In addition, the reducing environment created by long-term inundation can effectively suppress microbial decomposition, thereby promoting the accumulation of organic carbon at greater depths [52].

Sediment physicochemical properties and sediment carbon-related variables were analyzed for the CK and 20% thinning treatments only; the 40% thinning treatment was not included in sediment sampling. As a result, sediment responses under 40% thinning remain uncertain and warrant further evaluation in future work. We also acknowledge that the study is based on three replicate plots per treatment, which represents the lower bound for robust inference, particularly given the pronounced small-scale spatial heterogeneity of mangrove sediments. Therefore, the sediment-related findings should be interpreted with appropriate caution. It should also be noted that the two-year observation period in this study is relatively short for resolving long-term dynamics of sediment carbon storage and organic carbon burial. Carbon storage and organic carbon burial in mangrove ecosystems are complex processes driven by synergistic interactions between biotic factors and abiotic factors [53,54]. Therefore, its long-term trajectory will likely require longer-term monitoring to be robustly quantified. This study quantified changes in plant carbon density and sediment carbon density as separate carbon pools; however, an integrated ecosystem carbon balance was not constructed. Therefore, the present results do not allow a definitive assessment of whether thinning leads to a net gain or loss of total ecosystem carbon. This limitation is important because changes in aboveground and belowground biomass may offset, amplify, or lag behind changes in sediment carbon burial, and additional flux components (e.g., litter export, CO_2 efflux, and potential CH_4 emissions) were not measured. Accordingly, carbon storage and organic carbon burial in this study should be interpreted as pool-specific responses (plant biomass pool vs. sediment carbon burial/stock) observed over the two-year post-thinning period, rather than as a whole-ecosystem carbon budget. Long-term monitoring and a more comprehensive accounting of carbon stocks and fluxes would be required to determine the net ecosystem carbon consequence of thinning.

5. Conclusions

This two-year study evaluated short-term thinning effects on stand carbon density and sediment carbon burial indicators in an 8-year-old *K. obovata* mangrove plantation. Plant carbon density increased under thinning, with significantly higher values in the 20% and 40% treatments than in the unthinned control. In contrast, measured sediment carbon indicators (assessed only for CK and 20% thinning) declined over the same period, including decreases in sediment organic carbon content, sediment carbon density, and organic carbon burial rate relative to pre-thinning levels. Because sediment measurements did not include the 40% treatment and an integrated ecosystem carbon balance was not constructed, the net ecosystem carbon consequence of thinning cannot be determined from the present dataset, underscoring the need for longer-term monitoring with broader replication and sediment measurements across thinning intensities.

Author Contributions: Conceptualization, S.L. and J.W.; Methodology, J.W. and Q.C.; Software, S.L. and X.L.; Validation, S.L., X.L. and Q.C.; Formal analysis, S.L. and X.L.; Investigation, S.L., X.L., W.X., S.Y. and J.W.; Resources, J.W.; Data curation, S.L. and X.L.; Writing—original draft preparation, S.L.; Writing—review and editing, S.L., S.Y. and J.W.; Visualization, S.L. and J.W.; Supervision, S.Y.; Project administration, S.Y.; Funding acquisition, S.Y. All authors have read and agreed to the published version of the manuscript.

Funding: This research was funded by the Key Research and Development Program of Zhejiang Province (2023C02003), the Wenzhou High-Level Innovative Team Project (NY202401), and by the National Natural Science Foundation of China (31972864).

Data Availability Statement: The datasets used in this study are available from the corresponding author upon reasonable request.

Acknowledgments: The researchers express their sincere gratitude to those who created and publicly shared the data used in this study. Moreover, the researchers are grateful to Zhixia Zhao (Zhejiang Institute of Subtropical Crops) for her valuable assistance in revising the manuscript and improving the intellectual content of this work.

Conflicts of Interest: The authors declare no conflicts of interest.

Appendix A

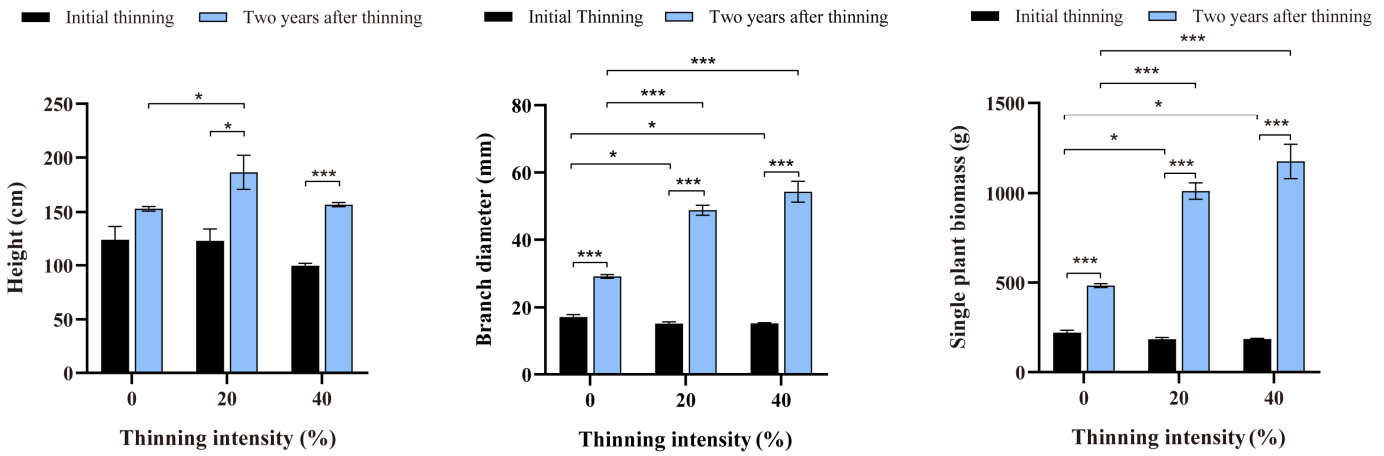


Figure A1. Differences in mangrove community structure under varying thinning intensities. Asterisks indicate significant pairwise differences as shown by the brackets (* $p < 0.05$, *** $p < 0.001$).

Table A1. Mangrove community structure at the initial thinning stage and two years after thinning under different thinning intensities.

Time Point	Thinning Intensity (%)	Height (cm)	Branch Diameter (mm)	Single Plant Biomass (g)
Initial thinning	0	123.6 ± 13.26	17.15 ± 0.71	222.21 ± 13.04
	20	122.47 ± 10.99	15.17 ± 0.54	185.53 ± 9.80
	40	99.63 ± 2.14	15.25 ± 0.16	187.37 ± 3.23
Two years after thinning	0	152.98 ± 2.11	29.13 ± 0.54	483.03 ± 10.88
	20	186.36 ± 15.62	48.96 ± 1.47	1010.63 ± 44.75
	40	156.73 ± 1.96	54.36 ± 3.03	1173.84 ± 94.33

Note: Values are means ± SE (n = 3 plots per treatment). 0% thinning intensity denotes the unthinned control (CK). Units are shown in column headers.

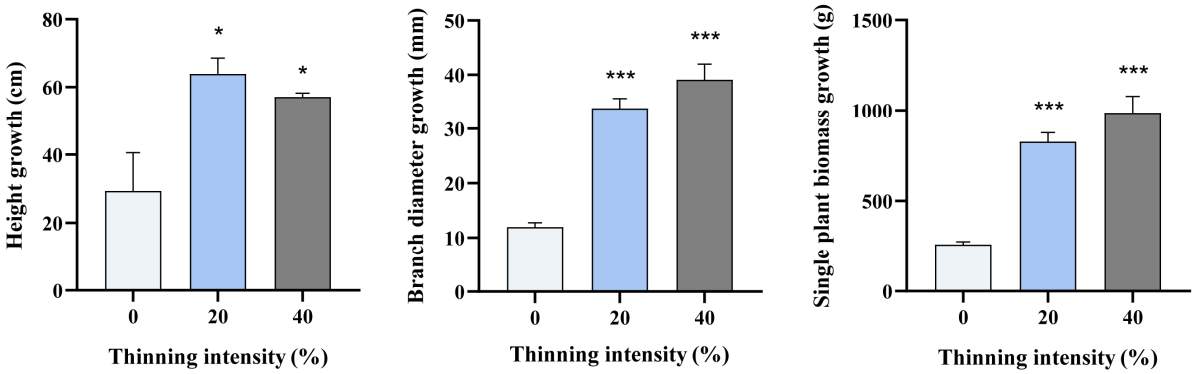


Figure A2. Effect of different thinning intensities on growth of *K. obovata* stands. Asterisks indicate significant differences compared with the control (* $p < 0.05$, *** $p < 0.001$).

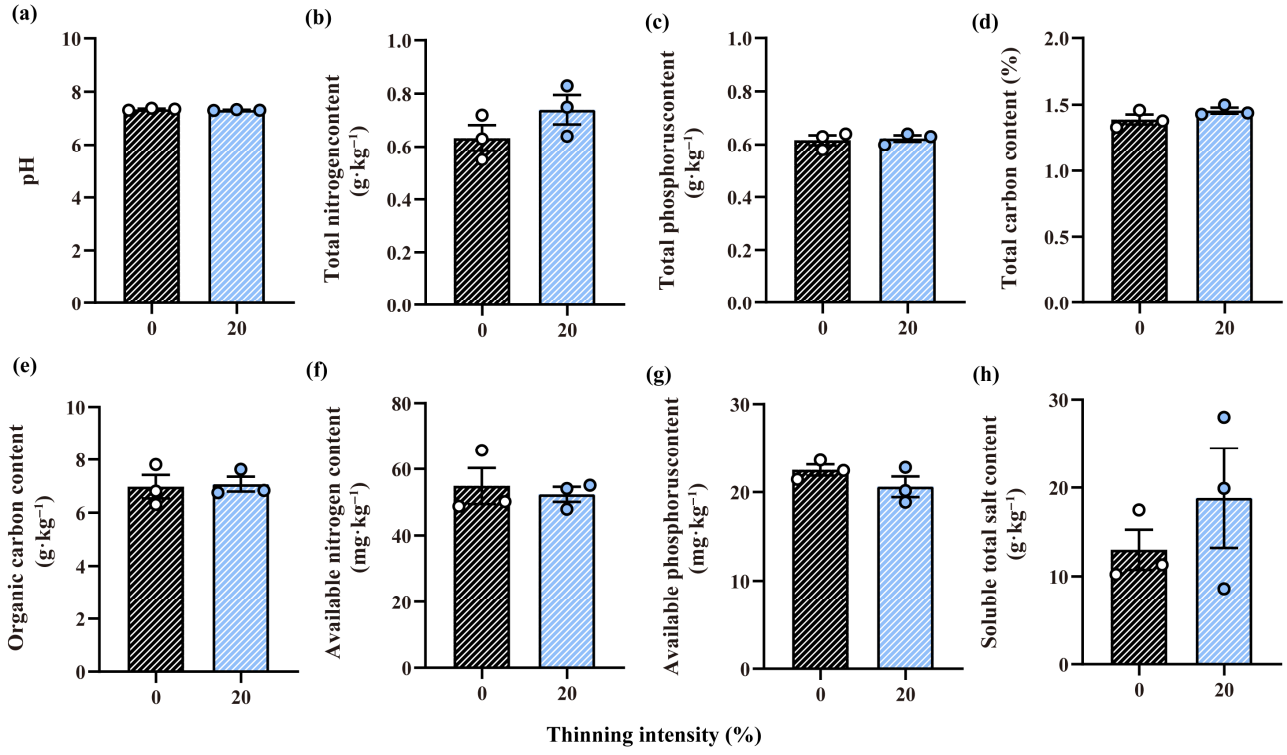


Figure A3. Physicochemical properties of *K. obovata* soil under moderate thinning. The circles represent individual data points (n = 3). No significant differences were detected among treatments. If no significant differences were detected for a variable, no letters are shown.

References

1. Pan, Y.; Birdsey, R.A.; Fang, J.; Houghton, R.; Kauppi, P.E.; Kurz, W.A.; Phillips, O.L.; Shvidenko, A.; Lewis, S.L.; Canadell, J.G.; et al. A large and persistent carbon sink in the world's forests. *Science* **2011**, *333*, 988–993. [CrossRef]
2. Keenan, R.J.; Reams, G.A.; Achard, F.; de Freitas, J.V.; Grainger, A.; Lindquist, E. Dynamics of global forest area: Results from the FAO Global Forest Resources Assessment 2015. *For. Ecol. Manag.* **2015**, *352*, 9–20. [CrossRef]
3. Chagnon, C.; Dumont, S.; Morin-Bernard, A.; Jactel, H.; Achim, A.; Moreau, G. Potential of thinning to increase forest resilience and resistance to drought, pest, windstorm and fire: A meta-analysis. *For. Ecol. Manag.* **2025**, *590*, 122788. [CrossRef]
4. Yan, T.; Zhu, J.; Fang, Y.; Yang, K.; Li, M. Effects of thinning on nitrogen status of a larch plantation, illustrated by ^{15}N natural abundance and N resorption. *Scand. J. For. Res.* **2018**, *33*, 357–364. [CrossRef]
5. Moreau, G.; Chagnon, C.; Achim, A.; Caspersen, J.; D'Orangeville, L.; Sánchez-Pinillos, M.; Thiffault, N. Opportunities and limitations of thinning to increase resistance and resilience of trees and forests to global change. *J. For. Res.* **2022**, *95*, 595–615. [CrossRef]
6. Clarke, N.; Kiær, L.P.; Kjønaas, O.J.; Bárcena, T.G.; Vesterdal, L.; Stupak, L.; Finér, L.; Jacobson, S.; Armolaitis, K.; Lazdina, D.; et al. Effects of intensive biomass harvesting on forest soils in the Nordic countries and the UK: A meta-analysis. *For. Ecol. Manag.* **2021**, *48*, 118877.
7. Ying, M.; Cheng, X.Q.; Kang, F.F.; Han, H.R. Effects of thinning on soil aggregation, organic carbon and labile carbon component distribution in *Larix principis-rupprechtii* plantations in North China. *Ecol. Indic.* **2022**, *139*, 108873. [CrossRef]
8. Li, X.; Li, Y.; Zhang, J.; Peng, S.; Chen, Y.; Cao, Y. The effects of forest thinning on understory diversity in China: A meta-analysis. *Land. Degrad. Dev.* **2020**, *31*, 1225–1240. [CrossRef]
9. Yang, J.J.; Yang, J.; Xiao, R.; Yang, K. Effects of thinning on promoting the growth and fruiting of *Pinus koraiensis* fruit forest. *For. Surv. Plan.* **2023**, *48*, 153–157+201.
10. Yang, L.; Zhao, C.H.; Xing, H.L.; Yang, L.; Shen, H.L. Effects of Thinning Intensity on the forest growth and stand accumulation of *Picea koraiensis* plantations. *J. Northwest For. Univ.* **2023**, *38*, 207–213.
11. Zhang, H.L.; Liu, S.R.; Yu, J.Y.; Li, J.W.; Shangguan, Z.P.; Deng, L. Thinning increases forest ecosystem carbon stocks. *For. Ecol. Manag.* **2024**, *555*, 121702. [CrossRef]
12. Ma, J.Y.; Kang, F.F.; Cheng, X.Q.; Han, H.R. Moderate thinning increases soil organic carbon in *Larix principis-rupprechtii* (Pinaceae) plantations. *Geoderma* **2018**, *329*, 118–128. [CrossRef]
13. Zhou, Z.H.; Wang, C.K.; Jin, Y.; Sun, Z.H. Impacts of thinning on soil carbon and nutrients and related extracellular enzymes in a larch plantation. *For. Ecol. Manag.* **2019**, *450*, 117523. [CrossRef]
14. Ma, J.Y.; Han, Y.; Ji, S.N.; Liu, B.; Lv, F.C.; Cai, X.; Du, J.Q.; Li, J.S. Reducing soil organic carbon mineralization under moderate thinning magnifies the soil carbon sink in a *Larix principis-rupprechtii* plantation. *CATENA* **2022**, *210*, 105858. [CrossRef]
15. Yang, S.Q.; Zhu, M.; Liu, X.D. Effects of thinning on fuel characteristics and carbon stock of *Robinia pseudoacacia* forest in Beijing Xishan Forest Farm. *Ecol. Sci.* **2018**, *37*, 94–100.
16. Yang, L.; Wang, J.S.; Geng, Y.; Niu, S.L.; Tian, D.S.; Yan, T.; Liu, W.G.; Pan, J.X.; Zhao, X.H.; Zhang, C.Y. Heavy thinning reduces soil organic carbon: Evidence from a 9-year thinning experiment in a pine plantation. *CATENA* **2022**, *211*, 106013. [CrossRef]
17. Chen, X.; Chen, H.Y.; Chen, X.; Wang, J.; Chen, B.; Wang, D.; Guan, Q. Soil labile organic carbon and carbon-cycle enzyme activities under different thinning intensities in Chinese fir plantations. *Appl. Soil Ecol.* **2016**, *107*, 162–169. [CrossRef]
18. Shen, Y.; Cheng, R.; Xiao, W.; Yang, S. Effects of understory removal and thinning on soil aggregation and organic carbon distribution in *Pinus massoniana* plantations in the Three Gorges Reservoir area. *Ecol. Indic.* **2021**, *123*, 107323. [CrossRef]
19. Murdiyarso, D.; Purbopuspito, J.; Kauffman, J.B.; Warren, M.W.; Sasmito, S.D.; Donato, D.C.; Manuri, S.; Krisnawati, H.; Taberima, S.; Kurnianto, S. The potential of Indonesian mangrove forests for global climate change mitigation. *Nat. Clim. Change* **2015**, *5*, 1089–1092.
20. Le, T.C. Studies on Landscape Dynamic, Structural Feature and Healthy Management Technology in Zhangjiang Mangrove Forest. Ph.D. Thesis, Chinese Academy of Forestry Sciences, Beijing, China, 2014.
21. Ning, Q.Y.; Huang, Z.J.; Lai, T.H.; He, B.Y.; Ma, R.Y.; Zhang, G.S.; Long, Y.Y.; Wei, Z.F.; Lin, J.L.; Li, Y.H.; et al. Quantitative dynamics of mangrove populations in Guangxi Shankou Mangrove Reserve. *J. Guangxi Acad. Sci.* **2024**, *40*, 248–257.
22. Wang, F.F.; Wu, G.J.; Yang, S.C.; Cao, W.Z. Characterizing storage and sources of soil organic carbon in estuarine mangrove wetlands. *Wetland Sci.* **2024**, *22*, 664–673.
23. Adame, M.F.; Cormier, N.; Taillardat, P.; Iram, N.; Rovai, A.; Sloey, T.M.; Yando, E.S.; Blanco-Libreros, J.F.; Arnaud, M.; Jennerjahn, T.; et al. Deconstructing the mangrove carbon cycle: Gains, transformation, and losses. *Ecosphere* **2024**, *15*, e4806. [CrossRef]
24. Lu, Z.; Qin, G.M.; Gan, S.C.; Liu, H.B.; Macreadie, P.I.; Cheah, W.; Wang, F.M. Blue carbon sink capacity of mangroves determined by leaves and their associated microbiome. *Glob. Change Biol.* **2024**, *30*, e17007. [CrossRef] [PubMed]
25. Lyu, C.C.; Ma, Y.D.; Shui, B.Y.; Yu, Y.; Li, B.; Li, X.L.; Zhong, Z.N.; Hu, C.Y. Burial, source characteristics and influencing factors of organic carbon in mangrove sediments at the mouth of the Oujiang River Estuary, China. *Acta Ecol. Sin.* **2024**, *35*, 2688–2696.

26. Liu, M.L.; Qi, Z.Y.; Zhu, M.D.; Chen, L.; Wang, P.; Xu, N.N. Study on the Population Structure and Dynamic Characteristics of *Kandelia obovata* in the North Marginal Introduction and Natural Distribution Region of Mangroves in China. *J. Ecol. Rural Environ. Sci.* 2025, *early publication*. [CrossRef]
27. Jin, C.; Wang, J.W.; Zheng, J.; Chen, Q.X.; Li, J.Q.; Lu, X. A assessment method of *Kandelia obovata* population biomass. *Acta Ecol. Sin.* **2012**, *32*, 3414–3422.
28. Wang, H.C.; Zhang, X.Q.; Zhang, J.G.; Qu, Y.C.; Ji, L. Variation of growth dominance in thinned Chinese fir stands with different planting densities. *For. Res.* **2021**, *34*, 32–38.
29. Kantavichai, R.; Turnblom, E.C.; Lowell, E.C. Effects of density control and fertilization on log wood quality from a douglas-fir stand in western oregon, USA. *For. Sci.* **2020**, *66*, 191–201. [CrossRef]
30. Pretzsch, H. Density and growth of forest stands revisited. Effect of the temporal scale of observation, site quality, and thinning. *For. Ecol. Manag.* **2020**, *460*, 117879. [CrossRef]
31. Hepner, H.; Lutter, R.; Tullus, A.; Kanal, A.; Tullus, T.; Tullus, H. Effect of early thinning treatments on above-ground growth, biomass production, leaf area index and leaf growth efficiency in a hybrid aspen coppice stand. *Bioenergy Res.* **2020**, *13*, 197–209.
32. Hu, Y.C.; Zhang, X.L.; Han, X.Y.; Wan, X.L.; Liang, T.M.; Lu, X.J. Responses of stand growth, regeneration, and understory species diversity in *Quercus mongolica* secondary forest to stand density. *Acta Ecol. Sin.* **2022**, *33*, 727–732.
33. Zheng, Y.; Feng, J.; Yu, S.H.; Bu, P.T.; Wang, Y.C.; Huang, X.; Zheng, L. Study on the forest growth and soil nutrient characteristics of *Larix* spp. plantations with different densities in mountainous area of Liaodong. *J. Cent. South Univ. For. Technol.* **2022**, *42*, 94–103.
34. Xiao, X.C.; Suo, H.J.; Li, C.Y.; Yang, Y.Z.; Peng, J.; Liu, Y.; Shi, L.; Li, J.W. Effects of thinning intensity on growth and stem form of middle-aged *Toona sinensis* plantation. *J. Cent. South Univ. For. Technol.* **2021**, *41*, 10–17.
35. Luo, Y.S.; Li, S.Y.; Jin, S.S.; Zhong, M.L.; Hu, C.W.; Yan, D.F. Effects of thinning on the spatial distribution heterogeneity of DBH and tree height in *Quercus variabilis* plantation. *J. Cent. South Univ. For. Technol.* **2023**, *43*, 104–112.
36. Matsushita, M.; Nishikawa, H.; Tamura, A. Effects of girdling intensity, pruning season and thinning on tree growth, crown vigor and wound recovery in Japanese larch. *Forests* **2022**, *13*, 449. [CrossRef]
37. Xue, L.; Pan, L.; Zhang, R.; Xu, P.B. Density effects on the growth of self-thinning *Eucalyptus urophylla* stands. *Trees* **2011**, *25*, 1021–1031. [CrossRef]
38. Li, S.Y.; Li, S.G.; Huang, M. Effects of thinning intensity on carbon stocks and changes in larch forests in China northeast forest region. *J. Res. Ecol.* **2017**, *8*, 538–544.
39. Liu, X.Y. Effects of Extreme Drought on Forest Carbon Storage and Carbon Sequestration Rate in Eastern Texas, USA. Master's Thesis, Shanxi Normal University, Xi'an, China, 2022.
40. Fu, X.C.; Chen, Y.J.; Huang, B.; Lei, J.; Yang, H.B.; Wen, J.; Du, P.Q.; Jiang, Z.M. Characteristics and differences of soils of bare flat, *Spartina alterniflora* community and artificial mangrove forest areas in Qi'ao lsland. *Wetland Sci.* **2022**, *20*, 715–720.
41. Huang, Z.X.; Wang, Y.; Guo, F.; Ouyang, X.G.; Zhu, Z.C.; Zhang, Y. Mangrove soil carbon stocks varied significantly across community compositions and environmental gradients in the largest mangrove wetland reserve, China. *Reg. Environ. Change* **2024**, *24*, 140.
42. Zhang, Y.; Meng, X.W.; Xia, P.; Zhang, J.; Liu, D.H.; Li, Z.; Wang, W.Z. Spatiotemporal variations in the organic carbon accumulation rate in mangrove sediments from the Yingluo Bay, China, since 1900. *Acta Oceanol. Sin.* **2021**, *40*, 65–77. [CrossRef]
43. Chen, L.Z.; Lin, Q.L.; Krauss, K.W.; Zhang, Y.; Cormier, N.; Yang, Q. Forest thinning in the seaward fringe speeds up surface elevation increment and carbon accumulation in managed mangrove forests. *J. Appl. Ecol.* **2021**, *58*, 1899–1909. [CrossRef]
44. Liu, X.; Xiong, Y.; Liao, B. Relative contributions of leaf litter and fine roots to soil organic matter accumulation in mangrove forests. *Plant Soil* **2017**, *421*, 493–503. [CrossRef]
45. Bassar, A.Z.; Dannoura, M.; Okada, N.; Kamruzzaman, M. Fine root dynamics of *Kandelia obovata*, *Rhizophora stylosa* and *Bruguiera gymnorrhiza* in a mangrove environment in Okinawa, Japan. *Reg. Stud. Mar. Sci.* **2023**, *64*, 103046. [CrossRef]
46. Li, B.; Shui, B.N.; Yu, Y.; Lv, C.C.; Li, X.L.; Shangguan, M.Z.; Wei, Z.; Hu, C.Y. Burial characteristics and source analysis of organic carbon in mangrove sediments, Yanpu Bay, China. *Acta Sedimentol. Sin.* **2025**, *43*, 2004–2014.
47. Chen, L.Z. Application of surface table for carbon budget assessment in coastal blue carbon ecosystems. *Oceanogr. Limnol. Sin.* **2022**, *53*, 261–268.
48. Xin, K.; Yan, K.; Li, Z.; Hu, J.L.; Qiu, M.H. Distribution of soil organic carbon in mangrove wetlands of Hainan Island and its influencing factors. *Acta Pedol. Sin.* **2014**, *51*, 1078–1086.
49. Lin, J.L.; Tian, Y.C.; Zhang, Y.L.; Bai, X.M.; Zhang, Q.; Tao, J.; Yang, Y.Z.; Yang, Y.W. Characteristics of spatial distribution of soil organic carbon in mangrove wetlands at the estuary of Maoling River, Beibu Gulf. *Mar. Environ. Res.* **2024**, *43*, 339–347.
50. Lin, Q.L.; Chen, L.Z.; Zhang, J.L.; Wang, L.C.; Yu, X.Y.; Guo, Q. How fine root turnover functions during mangrove root zone expansion and affects belowground carbon processes. *Plant Soil* **2023**, *488*, 451–463. [CrossRef]
51. Zhang, Y.S.; Xiao, L.; Guan, D.S.; Chen, Y.J.; Motelica-Heino, M.; Peng, Y.S.; Lee, S.Y. The role of mangrove fine root production and decomposition on soil organic carbon component ratios. *Ecol. Indic.* **2021**, *125*, 107525. [CrossRef]

52. Gong, J.; Liu, W.W.; Li, W.; Cui, L.J. Sediment organic carbon dynamics and accumulation in estuarine mangrove wetlands. *CATENA* **2025**, *259*, 109317. [CrossRef]
53. Ali, S.; Dey, G.; Nuong, N.H.K.; Rahman, A.; Wang, L.C.; Sukul, U.; Das, K.; Sharma, R.K.; Wang, S.L.; Chen, C.Y. Carbon sequestration in mangrove ecosystems: Sources, transportation pathways, influencing factors, and its role in the carbon budget. *Earth Sci. Rev.* **2025**, *269*, 105184. [CrossRef]
54. Kirwan, M.L.; Megonigal, J.P.; Noyce, G.L.; Smith, A.J. Geomorphic and ecological constraints on the coastal carbon sink. *Nat. Rev. Earth Environ.* **2023**, *4*, 393–406.

Disclaimer/Publisher's Note: The statements, opinions and data contained in all publications are solely those of the individual author(s) and contributor(s) and not of MDPI and/or the editor(s). MDPI and/or the editor(s) disclaim responsibility for any injury to people or property resulting from any ideas, methods, instructions or products referred to in the content.